J. Phytomed. Syn. Med. Bus. Chem. 1(1) (2021) 17-42

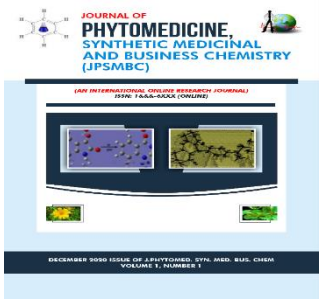

Journal of Phytomedicine, Synthetic Medicinal and Business Chemistry
(*An International Online Research Journal*)
journal homepage: www.craigobafoundation.com

Research Article

Cite this: **J. Phytomed. Syn. Med. Bus. Chem. 1(1) (2021) 17-42**
Publication Date: December, 2021
Document heading doi:

Antimalarial Screening and Molecular Docking Study of Some Bioactive Compounds from *Albizia zygia* Leaves for the Inhibition of Main protease (Mpro) of SARS-CoV-2 (COVID-19 Mpr °)

Adetola H. Adewole[a,*§], Olatomide A. Fadare[a], Ezekiel O. Iwalewa[b] and Craig A. Obafemi[a,*]

[a] Department of Chemistry, Faculty of Science, Obafemi Awolowo University, Ile-Ife, Nigeria

[b] Department of Pharmacology and Therapeutics, Faculty of Basic Medical Sciences, College of Medicine, University of Ibadan, Ibadan; Nigeria

[§] Current address: Department of Chemistry, University of Pretoria.

* Corresponding author.
E-mail address: ahadewole@gmail.com craigobafemi@gmail.com.

Article history:

Received 10 January 2021
Received in revised form 10 October 2021
Accepted 20 October 2021
Available online December, 2021

Abstract

Objective: Malaria and COVID-19 are two different diseases, but the first symptoms of malaria (including: fever, headache, and chills) are similar/common to symptoms of coronavirus disease 2019. This study was designed to isolate some phytochemicals from the hydroalcoholic extract of *Albizia zygia* leaves and assess their antimalarial activity and perform molecular docking studies to explore a possible inhibitor against plasmepsin II (a key enzyme in the life cycle of malarial parasite) and main protease of SARS-CoV-2 (a key enzyme contributing to the SARS-CoV-2 life cycle).

Methods: The 90% methanolic leaf extract of *Albizia zygia*, used in Nigerian folk medicine as remedy against arthritis, sprain and fever/malaria, was subjected to solvent partitioning and column chromatography analysis to obtain three known metabolites, a phytosterol and its phytosterone and glucopyranoside derivative (**1A**, **1B** and **2C**). Structures were confirmed by comparison of 1D and 2D spectral data with literature data.

Results: The crude extract and compound **2C** showed a level of antimalarial chemo-suppression which was a little lower than chloroquine (the standard drug used in this study) on early malarial infection. The molecular docking results indicated that in the case of plasmepsin II, the docked compounds have a lower binding affinity (-7.9, -8.0, -8.1 kcal/mol) relative to the native ligand (also a known inhibitor) (-9.9 kcal/mol) and also interacted less with the protein compared to the native ligand. However, the test compounds possess a better pharmacokinetic profile and may eventually possess some moderate antimalarial properties if administered orally. The glycosylated steroid **2C** exhibited the best binding affinity to the SARS-COV-2 main protease enzyme in terms of low binding energy (− 7.2 kcal/mol) (the native ligand had a binding energy of -6.1 kcal/mol) and the most polar contacts relative to the native ligand and other test ligands. **1A** and **1B** have binding energies of -6.3 and -6.5 kcal/mol respectively.

The observed better binding affinity of the test ligands compared to the known inhibitor (N3) (especially compound **2C** that has more polar interactions with the protein) suggests that the test compounds may be likely inhibitors of the SARS-COV-2 main protease and possible leads in the drug discovery effort for the management of the COVID-19 disease.

Conclusion: The research lends support to the ethnomedicinal use of the plant in combating malarial infections and shows the potential of its use in the treatment of COVID-19 infection and identification of leads for further drug discovery efforts.

Keywords: *Plasmodium berghei*; plasmepsin II; antimalarial; molecular docking

---

Introduction

Human beings have been using plants (in the form of decoctions, infusions, ointments, powders and syrups) as a source of medicines against a variety of diseases for many centuries [1, 2]. According to the World Health Organization (WHO) reports, about 80 % of populations in developing countries depend on traditional medicine based on bioactive compounds in plants mainly for their primary healthcare requirements [3].

Many medicinal plants have been subjected to scientific investigation for their various contributions to the healthcare system and in general their role and place in the strategies for the prevention of diseases [4, 5]. Bioactive compounds isolated from plants have been used for prevention or to treat a wide range of diseases such as inflammatory-, oncological-, pain- and parasitic-related diseases [4, 6-7].

Malaria, a parasitic, life-threatening disease, is most prevalent in the African region, particularly in sub-Saharan Africa, accounting for about 94% of malaria cases and 94% of deaths in 2019 [8]. The disease is preventable and curable. The first symptoms include fever, headache, and chills. These are similar/common to symptoms of the infectious disease, coronavirus disease 2019 (COVID-19), caused by a strain of coronavirus called severe acute respiratory syndrome coronavirus 2 (SARS-CoV-2). Thus, if symptoms alone are used to define a case, a malaria case may be classified incorrectly as COVID-19 and vice versa. The symptoms of malaria appear within 10-15 days after an infected female Anopheles mosquito bites a person, injecting *Plasmodium* parasite. Also common in severe cases among adults is multi-organ failure, while also expected in children with malaria is respiratory distress, similar to what is usually reported in patients with COVID-19 [9].

All countries are at very high risk of COVID-19. As at middle of December, 2021, over 273 million cases and over 5.3 million deaths have been reported globally, while in the African region, there are 11,029,265 cases with 9,846,953 recoveries and 239,627 deaths [10]. As of June 2021, WHO has approved the use of six COVID-19 vaccines, while other candidates are in the assessment pipeline. However, given the slow mass immunization efforts for developing (poor) countries [11], there is the need to continue to evaluate the potential use of

the constituents of medicinal plants as (complementary) interventions in COVID-19 management.

The genus *Albizia* belongs to the Mimosaceae plant family. It is native to tropical and subtropical regions of Asia and Africa and comprises of about 150 species which are mostly trees and shrubs [12]. In traditional medicine, different parts of *Albizia zygia* (bark, fruit, flowers and leaves) have been reported as useful medicinal remedies, especially for the management of painful conditions associated with tropical diseases. For example, the bark sap is used to treat inflammation of the eye (ophthalmia), while a decoction of its stem bark is used as an antidote, antiseptic, aphrodisiac, a purgative and for the treatment of stomach inflammation (gastritis), fever/malaria, parasitic worms and to overcome female sterility. In addition, the pounded bark is used to treat toothache and wounds, while the roots are used as an expectorant and the leaf decoctions are used to treat fever and diarrhea [13, 14, 15]. The plant parts have also been used to treat mental disorders [16].

In *Albizia zygia* pharmacological studies, both the non-polar (hexane) and polar (methanol) extracts from the plant stem bark exhibited antioxidant and antimicrobial activity [17], while its aqueous extract possesses anti-ulcer properties [18], the hydroethanol extract of the plant's roots demonstrated anti-oedemic, *in vivo* antioxidant, [19], antidepressant-like properties in animals [16, 19] and anticancer activity by showing a high selective toxicity against Jurkat cells [20]. The hydroethanol leaf extract possesses analgesic, anti-inflammatory, antipyretic properties [21] and exhibited antipsychotic-like activity [22] in animal models. The aqueous crude leaf extract of the plant possesses anti-diarrheal property and has inhibitory effect on gastrointestinal transit in rats [23], while the alcohol leaf and stem bark extracts have potent antioxidant and anti-inflammatory properties exhibited through different mechanisms [24, 25]. The methanolic extract of the stembark has been reported to exhibit strong antimalarial activity, (with an IC_{50} value of 1.04 µg/mL) [26].

Phytochemical investigation of the *Albizia zygia* afforded different classes of secondary metabolites such as alkaloids, flavonoids, glycosides, saponins, tannins and terpenes. Some compounds isolated and structurally identified from the plant were lupen-20(30)-3β-ol, 14α-Stigmast-5-en-3β-ol and 5α-Stigmast-7,22-dien-3β-ol, from the bark and leaves [27], albiziaprenol and phytol from the leaves [28]. In addition, some bioactive compounds isolated from the plant include two triterpenoid saponins from the roots (zygiaosides A–B) which dose-dependently induced apoptosis of human epidermoid cancer cell (A341) [29] and two new oleanane-type saponins, (zygiaosides C–D) [30], three flavonoids, 4′,7-dihydroxyflavanone, 3′,4′,7-trihydroxyflavone and 3′,4′,7-trihydroxy-3-methoxyflavone, were

isolated from the bark, with 3′,4′,7-trihydroxyflavone exhibiting high antimalarial activity (IC_{50} value 0.078 µg/ml, but displaying also cytotoxic effects (IC_{50} 0.405 µg/ml) against a cell line L6 [31].
Phenolic compounds from the leaves of the plant were found to show moderate activity against some human tumor cell lines and weak activity against *Plasmodium falciparum.* However, acetylation of quercetin 3-O-α-L-rhamnopyranoside, one of the two most abundant isolated compounds, gave two semi-synthetic derivatives, 2’’,3’’,4’’-triacetyl- and 2’’,3’’,4’’,7-tetraacetyl- derivatives, which exhibited significant activity against *P. falciparum* with IC_{50} values of 7.5 µM and 6.8 µM, respectively [32].

The main protease (Mpro) of SARS-CoV-2 plays a critical role in the COVID-19 disease propagation via processing the polyproteins which are necessary for its replication. The present study involved antimalarial screening and potential inhibitory action on COVID-19 protease of samples isolated from the aqueous methanol extract of *Albizia zygia* leaves.

2. Materials and methods

2.1. Plant material and preparation of plant extract

Fresh leaves of *A. zygia* were collected in the morning from Road 12, Obafemi Awolowo University Staff Quarters, Ile-Ife, Nigeria in September 2014. The plant was identified (with voucher specimen IFE-17607), authenticated and deposited at the Herbarium of the Department of Botany, Obafemi Awolowo University, Ile-Ife.

The leaves were air-dried at room temperature and ground into a fine powder, using a mechanical grinder (1.5 kg) and then macerated with methanol (90%) for 48 hours (repeated 2 times) at room temperature. Solvent was removed in vacuo from the combined filtered extract to give 73.0 g of crude extract. The resulting extract was stored in a refrigerator until it was needed.

2.2. Solvent partitioning of the crude extracts and isolation

The crude extract obtained was suspended in distilled water and separately partitioned in a 5 L separating funnel in turn with n-hexane (HEX), dichloromethane (DCM), ethyl acetate (EtOAc) and n-butanol (BuOH). This yielded four solvent fractions: n-hexane (8.1 g, 11.1 %), dichloromethane (7.0 g, 9.6 %), ethyl acetate (12.0 g, 16.5 %) and n-butanol (7.1 g, 9.7

%). The ethyl acetate fraction was chromatographed on silica gel (60-200 mesh) eluting with n-hexane 100% followed by an increasing gradient of ethyl acetate starting with 10% up to 100% ethyl acetate. This was followed with an increasing gradient of methanol from 10% in methanol up to 100% methanol. Test tube fractions (50 mL each) collected were monitored on TLC plates using Hexane/Ethyl acetate (1:2). Fractions having similar TLC characteristics were bulked together appropriately to afford seven sub-fractions (1A–1G). Sub-fraction 1A was concentrated, followed by addition of methanol (50 mL) and the mixture heated to give a clear solution and then left to stand at room temperature. This afforded an off-white solid (80 mg). This was further purified on silica gel column using hexane/ethyl acetate (90:10) and (80:20). Test tube 3–12 showed single spots on TLC, this yielded a mixture of compounds **1A** (major) and **1B** (minor).

From sub-fraction 1C was obtained a yellowish solid. This was washed twice with methanol and then recrystallized from ethanol/petroleum ether to give a white solid, **2C** (62 mg).

2.3. Animals and Ethical Approval

Swiss albino mice of both sexes (18–22 g) were used. The animals were well cared for under standard laboratory conditions. The animals were provided free access to standard commercial diet and water ad libitum (22° ± 3 °C) and acclimatized for 1 week before the beginning of the experiment. The experimental procedures were approved by the Animal Care and Use Research Ethics Committee and performed in accordance with the National Institute of Health/National Research Council. Guide for the care and use of laboratory animals. 8th ed; 1996.

2.4. Parasite and Infection

For the *in vivo* antimalarial assay, a chloroquine-tolerant *Plasmodium berghei* (strain NK 65), a rodent malaria parasite, was used. The blood-stage CQ-tolerant-induced parasite, was obtained from Institute for Medical Research and Training (IMRAT), University College Hospital (UCH), Ibadan, Nigeria. A standard inoculum of 1×10^7 of parasitized erythrocytes from a donor mouse was used to infect the experimental animal intra-peritoneally.

2.5. Evaluation of the Suppressive Antimalarial Activity: 4-Day Suppressive Test

Plasmodium berghei four-day suppressive test, which is the most widely used preliminary test, is used to measure the efficacy of four daily doses of test compounds by comparison of blood parasitemia and survival times of treated and untreated mice. The test compounds are

the isolated compound **2C,** the crude extract and butanol fraction and compare their anti-plasmodial effect with chloroquine (standard).

Parasitized erythrocytes were obtained from a donor infected mouse of 26% parasitemia, by cardiac puncture with a sterile needle and syringe. The inoculum was prepared by diluting the infected stock mice blood with saline solution. Forty-four (44) mice were selected and inoculated intra-peritoneally with the blood suspension (0.2 mL) containing infected erythrocytes on the first day of the experiment (D_0). The mice were randomly divided into eleven (11) groups, with each group consisting of 4 animals. Groups 1, 2 and 3 receiving correspondingly doses of 10, 50 and 100 mg/kg of isolated compound **2**C. Groups 4, 5, 6 and groups 7, 8, 9 also received 10, 50 and 100 mg/kg of the butanol fraction and the crude extract, respectively. Chloroquine diphosphate at 10 mg/kg was administered to the animals in group 10 (positive control) and to the animals in negative control (group 11), 0.2 mL of the vehicle used to administer the selected extracts and isolated compounds, DMSO, was administered. Administration was for four consecutive days (D_0 to D_3).

On the fifth day (D_4) after administration of parasite inoculum, blood was collected from the tail of each mouse [33] and smeared on to a microscope slide to make a thin film. The blood films were fixed with methanol, stained with Giemsa at pH 7.2 for 12 hours and the parasitemia was examined microscopically with 100-x magnification (oil immersion). The percentage chemo-suppression caused by the test extracts and isolated compound was calculated by comparing the parasitemia of the infected controls with those of the test mice treated with either the selected extracts or the isolated compound [34, 35]. The survival time in days was also recorded and survival index determined for each group.

The percentage parasitemia was estimated as a count of parasitized red blood cells divided by the total red blood cells counted within ten microscope fields:

$$\%\ Parasitemia = \frac{Parasitized\ red\ blood\ cells}{Total\ red\ blood\ cells} \times 100$$

The percentage chemo-suppression was calculated as a relative value taking into account the percentage parasitemia of the negative control (the group of animals infected with the parasite but were not administered any drug). The formula used is as described below:

$$\%\ Chemosuppression = \frac{(X - Y)}{X} \times 100$$

$$where\ X = \%\ Parasitemia\ of\ negative\ control$$

$$and\ Y = \%\ Parasitemia\ of\ test\ compound$$

2.6. Survival Time and Indices in a 4-day Test

The survival indices of the experimental animals for each of the test compounds are presented as a relative value (in percentage), taking into consideration the survival time of the negative control group of animals and the survival time of the experimental animals. The survival indices (in percentage) of the experimental drugs were calculated using the formula;

$$Survival\ index\ (\%) = \frac{(A - B)}{(28 - B)} \times 100$$

$$Where\ A = last\ day\ of\ animal\ with\ test\ drug$$

$$and\ B = last\ day\ of\ animal\ without\ drug\ (negative\ control).$$

2.7. Molecular Docking and ADME Prediction

The coordinates of the target proteins were retrieved from the protein data bank (5YIA for plasmepsin II and 6LU7 for SARS-COV-2 main protease) and edited with the pymol software to remove water of crystallization and other bound small molecules. The bound inhibitor for each protein was also processed and saved to be used as reference for the docking study (Figure 4). The study ligands (Figure 1) 3D structure was generated using the Chem 3D software, energy minimized and saved in the pdb format. The saved protein files were processed further with the AutoDock tools, a grid box was set up centered around the active site of the proteins (the active site was taken to be the pocket occupied by the native inhibitors) and the protein was saved in the pdbqt format. The study ligands and extracted bound inhibitors were also processed further with the AutoDock tools and saved in the pdbqt format. The pdbqt files for proteins and ligands were used for the molecular docking calculation with the Autodock Vina program [36,37]. The test compounds and reference compounds were also saved as .sdf files and uploaded to the preADMET server (South Korea) for in-silico ADME prediction. Parameters such as human intestinal absorption (HIA), Cell permeability (Caco2 model), plasma protein binding (PPB), P-glycoprotein interaction (Pgp), Cytochrome P450 enzyme (CYP3A4) interaction and blood brain barrier penetration (BBB) were predicted.

3.0. Results

3.1. Compounds 1A and 1B

IR spectrum (KBr, cm^{-1}) for the mixture of **1A and 1B** showed absorption bands for O-H stretching frequency at 3423, aliphatic groups at 2918 and 2859, C=O stretching frequency at

1718 (medium intensity), C=C stretching frequency at 1654 (weak intensity), $–CH_3$ or $–CH_2–$ bending frequency at 1464 and 1381 and C–O stretching at 1060 (medium intensity). Further structure determination of **1A and 1B** was by ^{1}H-NMR, ^{13}C-NMR, DEPT 90, DEPT 135, HSQC and COSY and comparison with literature data. The ^{1}H and ^{13}C-NMR chemical shift data are given in Table 1, showing only the important diagnostic signals in the ^{1}H NMR. The signal at δ 3.50 is diagnostic of the sterol H-3. Two alkene proton signals appearing at δ 5.0 and 5.1 which are identical with the chemical shift of H-22 and H-23, respectively. The signal corresponding to the alkene proton H-6 appears further downfield as a triplet at δ 5.33.

The ^{13}C spectrum accounted for the alkene carbons of C-5, C-6, C-22 and C-23 at δ_C 140.73, 121.72, 138.32 and 129.24 ppm respectively. C-5 was confirmed as a quaternary since the signal at δ_C 140.73 was absent on both DEPT 90 and 135 spectra. The carbon signal at δ_C 207.08 represents C-3 when it is in the ketone form. The HSQC spectrum helped in the correlation of the ^{1}H and ^{13}C values. The structures of the mixture were therefore proposed as stigmast-5,22-dien-3-ol (**1A)** and 24-ethylcholest-5,22-dien-3-one (**1B)** (stigmasterone).

Compound **2C** was isolated as a white powder with melting point of 287-288 °C (dec.). Its infrared spectrum (KBr, cm $^{-1}$) showed absorption bands at 3360 (-OH), 2957, 2931, 2866 (sp^3-CH), 1669 (w, C=C), 1459, 1380 (CH_3/CH_2), 1105, 1051, 1019 (C-O).

The ^{1}H-NMR (DMSO-d_6) of **2C** showed signals between δ 5.31 and 0.75, with one alkene proton at δ 5.31 (H-6), two protons with substituted alkene at δ 5.10 (H-22) and 5.00 (H-23) and one anomeric proton on C-1'at δ 4.21. The ^{13}C-NMR spectrum of the compound showed 35 signals at δ_C: 23.86, 28.67, 55.32, 12.02, 19.02, 41.74, 19.63, 138.06, 128.21, 50.59, 31.36, 20.97, 21.17, 22.48, 36.82, 31.41, 76.88, 36.82, 140.44, 121.23, 31.34, 29.26, 49.58, 36.21, 21.18, 38.29, 41.85, 56.26, 12.30, 100.76, 73.45, 76.75, 70.07, 76.87, 61.07 ppm. The comparison of the ^{13}C spectral data for the stigmasterol glycoside with literature values are given in Table 2.

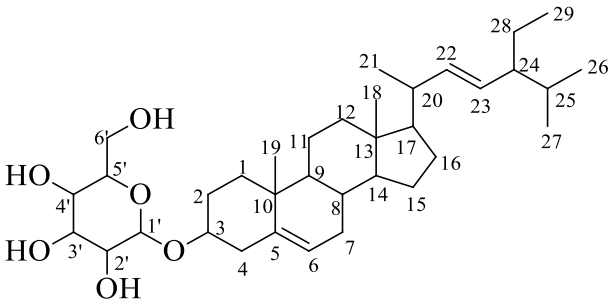

stigmast-5,22-dien-3-*O*-glucopyranoside (2**C)**

Table 1: Comparison of ^{1}H and ^{13}C-NMR spectral data of mixture of compounds **1A and 1B** with literature values for stigmasterol and stigmasterone

Position	Experimental		Stigmasterol[a]		Stigmasterone[b]
	^{1}H	**^{13}C**	**^{1}H**	**^{13}C**	**^{13}C**
1		37.23		37.6	35.9
2		31.63		32.1	34.2
3	3.50 (s, 1H)	71.80 (207.05)	3.51 (tdd, 1H)	72.1	200.57
4		42.27		42.4	124.45
5		140.73		141.1	172.62
6	5.33 (t, 1H)	121.72	5.31 (t, 1H)	121.8	33.70
7		33.91		31.8	32.77
8		30.94 (36.13)		31.8	36.33
9		50.12 (55.92)		50.2	54.53
10		36.49		36.6	39.34
11		21.05		21.5	21.75
12		39.65		39.9	40.34
13		44.84		42.4	43.11
14		56.84		56.8	56.59
15		25.40		24.4	24.92
16		28.92		29.3	28.94
17		56.02		56.2	56.71
18		12.38		12.2	12.72
19		19.74		18.9	18.11
20		40.50		40.6	41.24
21		20.09		21.7	21.86
22	5.0 (m, 1H)	138.32	4.98 (m, 1H)	138.7	138.89
23	5.1 (m, 1H)	129.24	5.14 (m, 1H)	129.6	130.15
24		45.80 (51.22)		46.1	51.97
25		29.11 (31.89)		29.6	32.61
26		21.84		20.2	19.76
27		20.96		19.8	21.91
28		26.02		25.4	26.16
29		12.40		12.1	13.01

The stigmasterone isolated in [39] is D4-stigmasterone

a: [38] b: [39]

Table 2: Comparison of ^{13}C spectra data of compound **2C** with literature values for stigmasterol glycoside

Position	Experimental	Literature[a]	Literature[b]
1	36.82	37.36	38.28
2	31.41	31.94	33.33
3	76.88	77.43	76.95
4	36.82	36.69	36.76
5	140.44	140.99	140.43
6	121.23	121.72	121.04
7	31.34	29.79	31.30
8	29.26	31.99	31.38
9	49.58	50.15	49.57
10	36.21	36.77	36.15
11	21.18	21.65	22.59
12	38.29	38.84	41.68
13	41.85	42.28	41.80
14	56.26	55.86	56.20
15	23.86	24.42	24.72
16	28.67	29.05	29.20
17	55.32	56.79	56.11
18	12.02	12.39	11.76
19	19.02	19.39	18.99
20	41.74	40.03	35.37
21	19.63	21.49	18.76
22	138.06	138.59	137.85
23	128.21	129.35	128.79
24	50.59	51.12	31.20
25	31.36	31.87	31.20
26	20.97	21.18	19.28
27	21.17	19.64	18.89
28	22.48	25.58	23.76
29	12.30	12.67	11.58
1’	100.76	101.29	100.77
2’	70.07	70.62	70.14
3’	76.75	77.28	76.75
4’	73.45	73.99	73.43
5’	76.87	73.08	76.63
6’	61.07	61.61	61.10

a: [40] b: [41]

3.2. 4-day suppressive test

The antiplasmodial activity of varying oral doses of the crude methanolic extract (CE), butanol fraction (BF) and isolated compound **2C** compared to chloroquine during an early *P. berghei* infection (4-day test) in mice is shown in Table 3 (Figure 1).

Table 3: Chemosuppressive ability of the different levels of treatment on early malaria

Treatment	Dose (mg/kg)	% Parasitemia	% Chemosuppression
Control (NC)	-	3.09 ± 1.32	0
Chloroquine (PC)	10	0.66 ± 0.25	78.64
CE	10	1.42 ± 0.01	54.05
	50	1.42 ± 0.74	54.05
	100	1.14 ± 0.46	63.11
BF	10	2.47 ± 0.43	20.06
	50	1.41 ± 0.21	54.37
	100	1.62 ± 0,04	47.57
2C	10	2.09 ± 0.32	32.36
	50	1.66 ± 0.64	46.28
	100	1.29 ± 0.21	58.25

Values are mean ± standard error
Legend: **NC** – Negative control, **PC** – Positive control, **CE** – Crude extract, **BF** – Butanol fraction, **2C** – Isolated glycoside

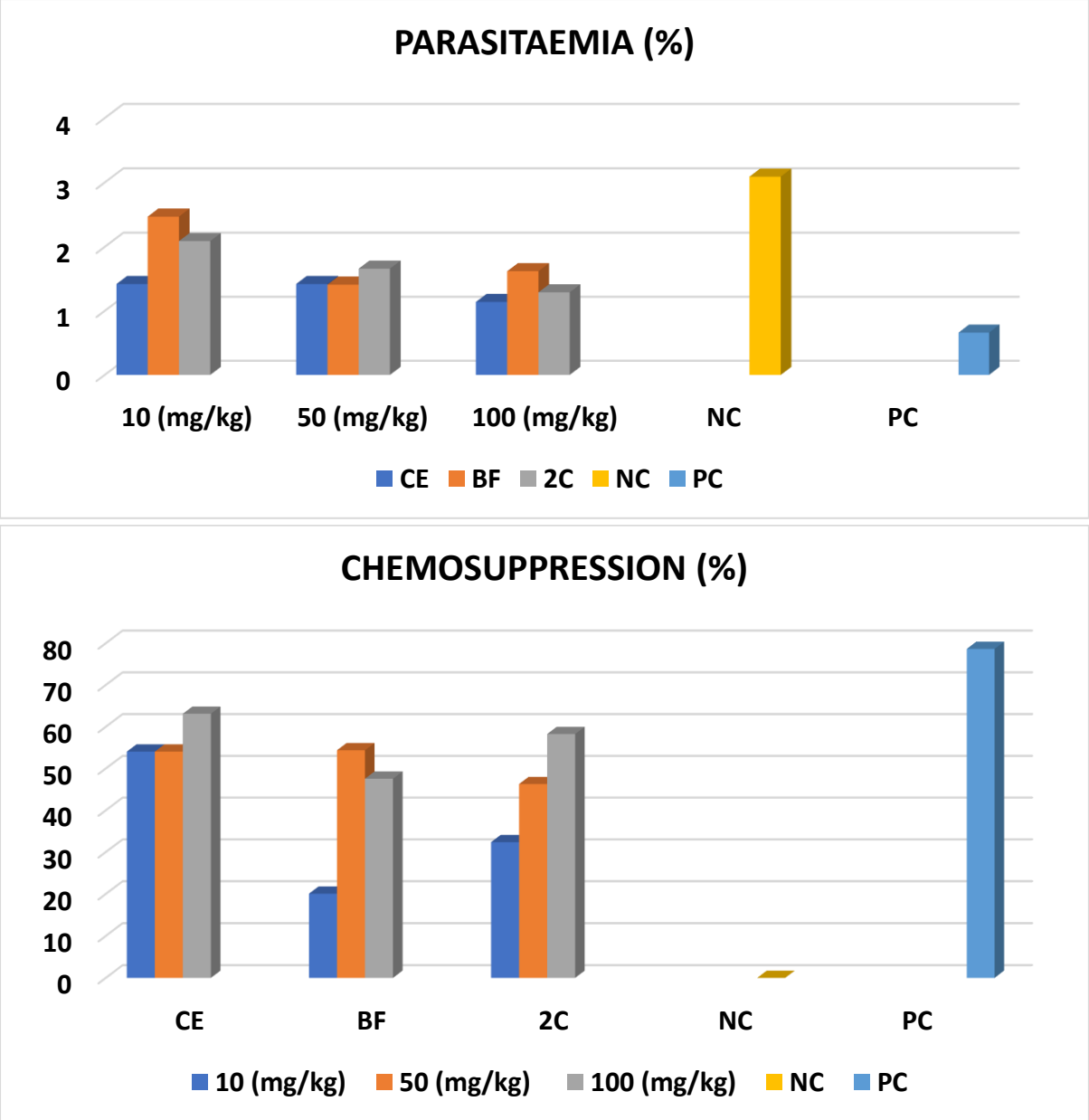

Figure 1. Histogram for the antimalarial activity.

3.3. Survival Time and Indices in a 4-day Test

The survival indices of the experimental animals for each of the test compounds are presented as a relative value (in percentage), taking into consideration the survival time of the negative control group of animals and the survival time of the experimental animals. The mean survival time (days) and the survival index of the mice treated with the selected extracts and isolated compound C in an early *P. berghei* infection are given in Table 4 (Figure 2).

3.4. Molecular docking

To predict the potential interactions of compounds **1A, 1B** and **2C (**Figure 1) with SARS-COV-2 main protease and plasmepsin II, molecular docking calculations were performed. The binding affinity and their interacting residues and polar contacts of ligands are given in Tables 5 and 6.

The predicted pharmacokinetic properties of the study compounds are given in Table 7.

Table 4. Mean survival period and survival index of test animals with the different levels of treatment in early malaria infection test.

Treatment	Dose (mg/kg)	Survival time (days)	Survival index (%)
Control (NC)	-	9.7	-
Chloroquine (PC)	10	21.0	61.75
CE	10	17.3	41.53
	50	14.0	23.50
	100	13.3	19.67
BF	10	11.3	8.74
	50	13.7	21.86
	100	16.0	34.43
2C	10	10.0	1.64
	50	17.7	43.72
	100	20.3	57.92

Legend: **NC** – Negative control, **PC** – Positive control, **CE** – Crude extract, **BF –** Butanol fraction, **2C** – Isolated glycoside

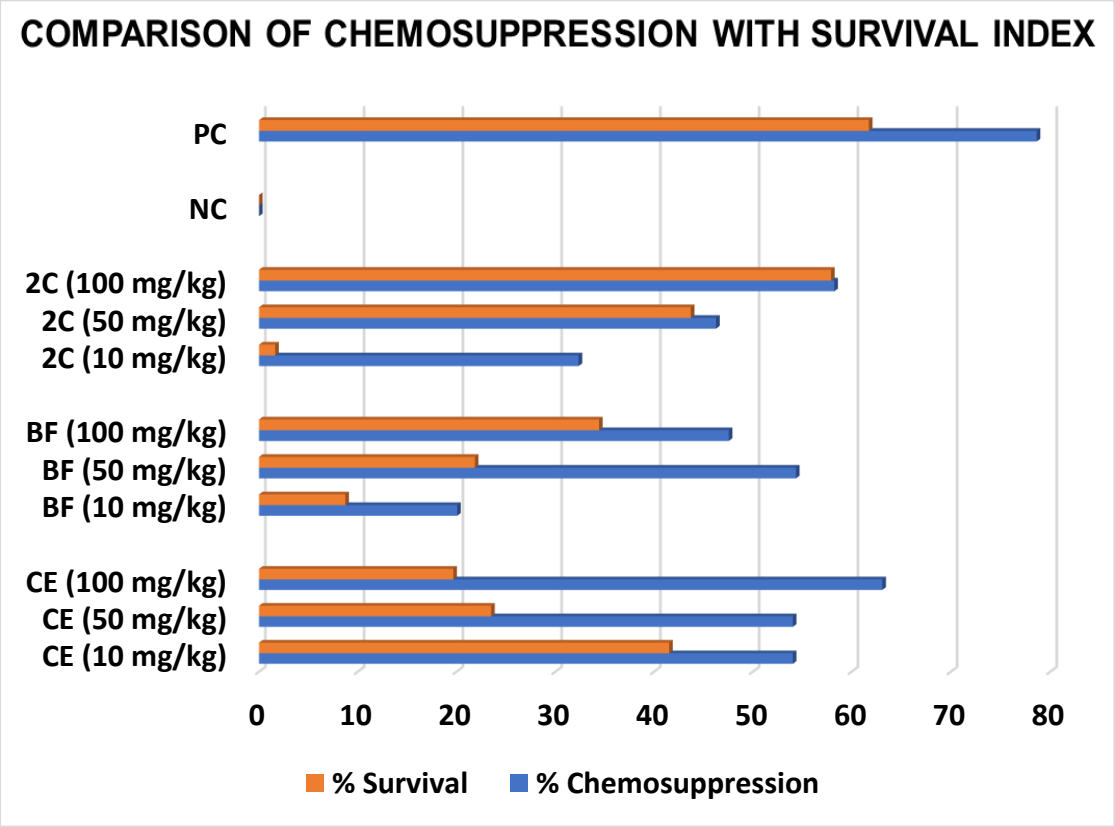

Figure 2. Histogram of percentage chemo-suppression compared with survival index

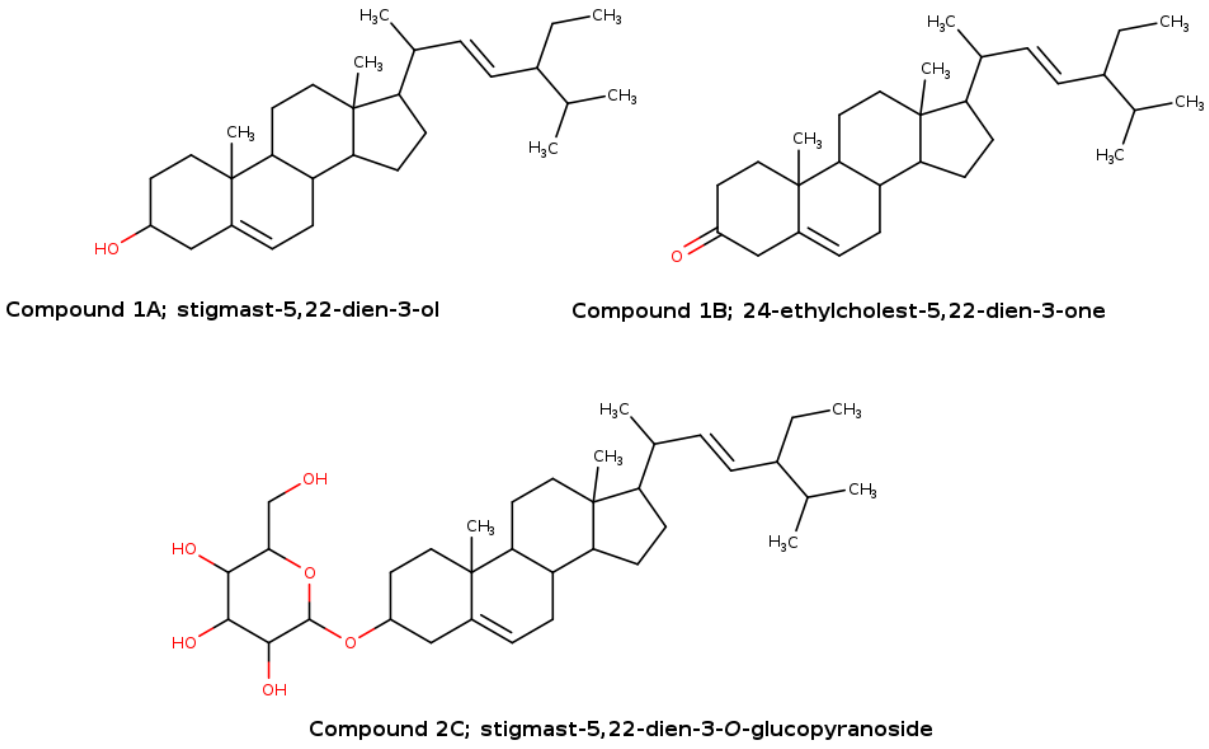

Figure 3. Structures of the study compounds

TABLE 5: Binding energy and interactions of ligands with SARS-COV-2 main protease

Compound	Binding Affinity (-kcal/mol)	Interacting residues (SARS-COV-2 MAIN PROTEASE)	Polar contacts
1A	6.3	LEU141, ASN142, GLY143, SER144, CYS145, HIS163, HIS164, MET165, GLU166, ARG188, GLN189, THR190	3 polar contacts
1B	6.5	LEU141, ASN142, CYS145, HIS163, HIS164, MET165, GLU166, LEU167, PRO168, GLN189, THR190, ALA191, GLN192	1 polar contact
2C	7.2	HIS41, MET49, LEU141, ASN142, GLY143, SER144, CYS145, HIS163, HIS164, MET165, GLU166, LEU167, PRO168, GLN189	4 polar contacts
N3	6.1	THR25, THR26, LEU27, HIS41, SER46, MET49, PHE140, ASN142, GLY143, CYS145, HIS163, HIS164, MET165, GLU166, HIS172, ARG188, GLN189	3 polar contacts

TABLE 6: Binding energy and interactions of ligands with plasmepsin II

Compound	Binding Affinity (-kcal/mol)	Interacting residues (PLASMEPSIN II)	Polar contacts
1A	7.9	ASP36, GLY38, TYR79, VAL80, LEU133, TYR194, ILE214, ASP216, GLY218, THR219, LEU294, ASP295, PHE296, ILE302	1 polar contact
1B	8.0	ASP36, GLY38, TYR79, VAL80, SER81, TYR194, ILE214, ASP216, GLY218, THR219, SER220, ALA221, PHE301	No polar contacts
2C	8.1	MET17, ILE34, ASP36, GLY38, TYR79, VAL80, SER81, THR116, TYR194, ILE214, ASP216, GLY218, THR219, SER220, LEU294, ASP295, PHE296,	1 polar contact
8V9	9.9	ILE34, ASP36, GLY38, ASN78, TYR79, VAL80, SER81, ILE125, LEU133, TYR194, ILE214, ASP216, GLY218, THR219, SER220, ALA221, THR223, ILE292, PHE296, ILE302	9 polar contacts

TABLE 7: Predicted pharmacokinetic properties of the study compounds

Compound	BBB	HIA	PPB	Caco2	Pgp	CYP3A4_i	CYP3A4_s
1A	19.89	100	100	52.34	Inhib[#]	i*	s**
1B	20.09	100	100	54.17	Inhib	I	S
2C	4.42	90.57	100	25.16	Inhib	I	S
N3	0.043	78.74	81.30	21.00	Inhib	I	S
8V9	0.042	86.88	90.77	18.02	Non	I	S

*** inhibitor of CYP3A4** **[#] Inhibitor of Pgp**

****substrate of CYP3A4**

4.0. Discussion

The mixture of compounds **1A** and **1B**, isolated as an off-white powder, tested positive for steroids using the Salkowski reaction as described by Harborne [42]. Compounds **1A** and **1B** were compounds identical to stigmast-5,22-dien-3-ol (stigmasterol) and 24-ethylcholest-5,22-dien-3-one (stigmasterone) respectively, based on the analysis of the FTIR, ^{1}H NMR, ^{13}C NMR (Table 1) and HSQC data, as well as by comparison with published data.

The ^{1}H NMR spectrum of compound **2C** showed the glycosidic protons at positions 2', 3', 4', 5' and 6' at δ_H 2.9 – 3.6, while the OH protons at 2', 3' and 4'overlapped between δ_H 4.6 to 4.9 and the triplet appearing at δ_H 4.42 was due to the proton 6'-OH.

Signals characteristic of a glucopyranoside was observed on the ^{13}C spectrum (Table 2). An anomeric carbon appearing at δ_C 100.76 ppm indicated the presence of a single glucopyranoside entity. Of the six sugar carbon signals, there were four oxygenated methine (CH) resonances at δ_C 70.81, 73.45, 76.75 and 76.87 ppm, one oxygenated methylene (CH_2) resonance at δ_C 61.07 ppm. Alkene carbon signals were observed at δ_C 140.44 (C-5), 121.23 (C-6), 138.06 (C-22) and 128.21 (C-23). C-5 at 140.44 was confirmed to be a quaternary carbon due to the absence of the signal on the DEPT 90 and 135 spectra.

The antimalarial activity of the crude extract of the leaves of *Albizia zygia*, used in traditional medicine in Nigeria and elsewhere in Africa, against *Plasmodium berghei* infection in mice in four-day suppressive test model is reported.

The crude methanolic extract produced a dose dependent chemosuppressive effect. A compound is taken to be active when percent suppression in parasitemia is 30 % or more [43]. The average percentage suppression of parasitemia observed in the mice treated with the

crude extract were 54.05, 54.05, and 63.11 % at the doses of 10, 50 and 100 mg/kg per day, respectively, as compared to negative control. Chloroquine at 10 mg/kg per day produced 78.64 % chemo-suppression. The lowest effective dose for the crude extract from this experiment was 10 mg/kg per day. On the other hand, the butanol fraction did not produce a dose dependent chemo-suppressive effect. The average percentage suppression of parasitemia were 20.06, 54.37 and 47.57 % at doses of 10, 50 and 100 mg/kg per day, respectively.

A dose dependent chemo-suppressive effect was noticed in isolated compound 2C. The average percentage suppression of parasitemia were 32.36, 46.28 and 58.25 % at doses of 10, 50 and 100 mg/kg per day, respectively. This showed a steady increase in the chemo-suppressive ability of 2C as the dose increased. The butanol fraction is however relatively low compared to the crude extract and 2C in terms of its chemo-suppressive potential.

Despite the effectiveness of the crude extract in suppression of parasites in early malaria, it appears to be toxic. The survival index of the Swiss albino mice treated with CE during the 28-day experiment revealed that as the dose increased, the survival time reduced. Mice treated with CQ at 10 mg/kg per day survived for 21.0 days whereas, those treated with CE at 10, 50 and 100 mg/kg per day survived for 17.3, 14.0 and 13.3 days respectively. The negative controlled group had a mean survival time of 9.7 days.

Isolated compound **2C** appears to be less toxic compared to other treatment carried out in this early malaria test. As the dose increased, the chemo-suppressive ability increased and even the mean survival time increased. The mean survival time of the mice treated with 2C at 10, 50 and 100 mg/kg per day survived for 10.0, 17.7 and 20.3 days respectively. The butanol fraction also appears to be less toxic considering the fact that as the dose increased, the mean survival time also increased. The chemo-suppressive ability however was not commeasurable in its increase. Animals treated with butanol fraction at 10, 50 and 100 mg/kg per day survived for 11.3, 13.7 and 16.0 days respectively.

Regarding docking, the predicted binding energy is calculated. A stronger binding is indicated by a more negative binding energy [44]. The docked ligands in the SARS-COV-2 main protease occupied the same space as the native ligand (also a known inhibitor) and interacted with similar amino acid residues within the binding site (Figure 4). The native ligand had a binding energy of -6.1 kcal/mol which was lower than that estimated for the three test ligands. The binding energy of the other test ligands ranged from -6.3 to -7.2 kcal/mol (Table 5). The glycosylated steroid had the highest binding energy and the most polar contacts relative to the native ligand and other test ligands. The observed binding energy

of the test ligands being higher than those of the known inhibitor (especially the compound 2C that has more polar interactions with the protein) suggests that the test compounds may be likely inhibitors of the SARS-COV-2 main protease and possible leads in a drug discovery effort for the management of the COVID-19 disease by virtue of the fact that the compounds have the pharmacokinetic properties that would aid bio-availabilty if administered orally. The test compounds are predicted to have high human intestinal absorption (Table 3) and moderate cell permeability (Caco 2 model). The compounds are also predicted to be inhibitors of CYP3A4 (though substrates to CYP3A4 as well) which may prevent the compounds from being rapidly metabolized during the first pass thus facilitating bioavailability.

In the case of plasmepsin II, the docked compounds have a lower binding affinity (Table 6) relative to the native ligand (also a known inhibitor). The test compounds also interacted less with the protein compared to the native ligand (Figure 5). Compound 1B had no polar contact while the other two compounds had one polar contact with the protein. It is therefore, likely that the test compounds may not be as potent at inhibiting the plasmepsin II compared to the native ligand. The test compounds however, having a better pharmacokinetic profile may eventually possess some moderate antimalarial properties if administered orally.

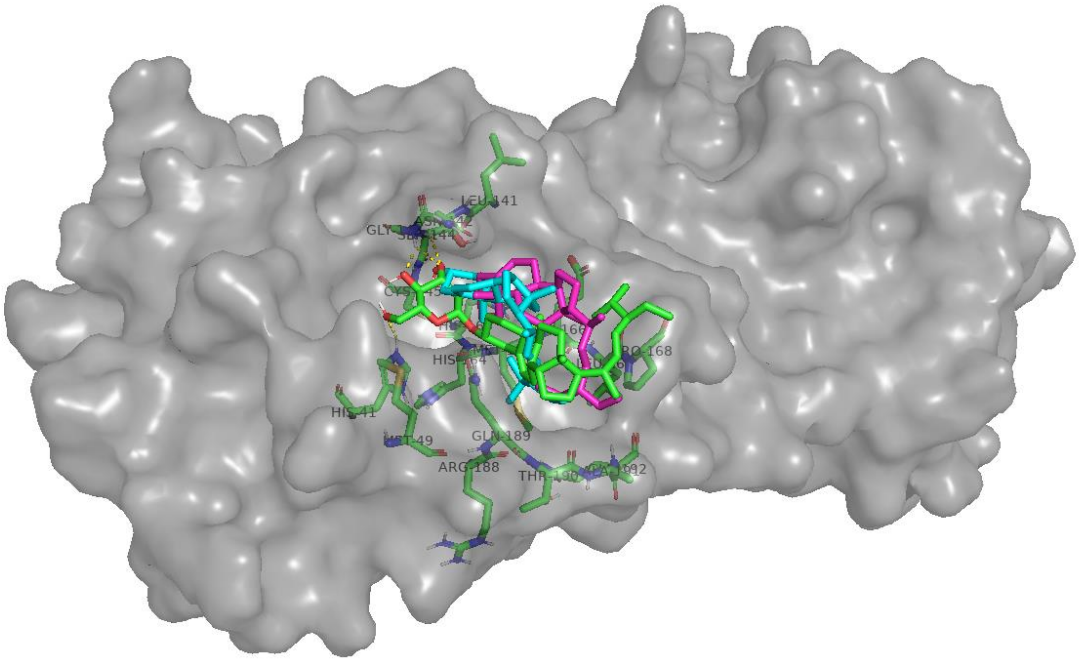

Figure 4: Compounds **1A** (cyan), **1B** (magenta) and **2C** (green) bound to SARS-COV-2 main protease. The compounds assume different conformations within the same cavity.

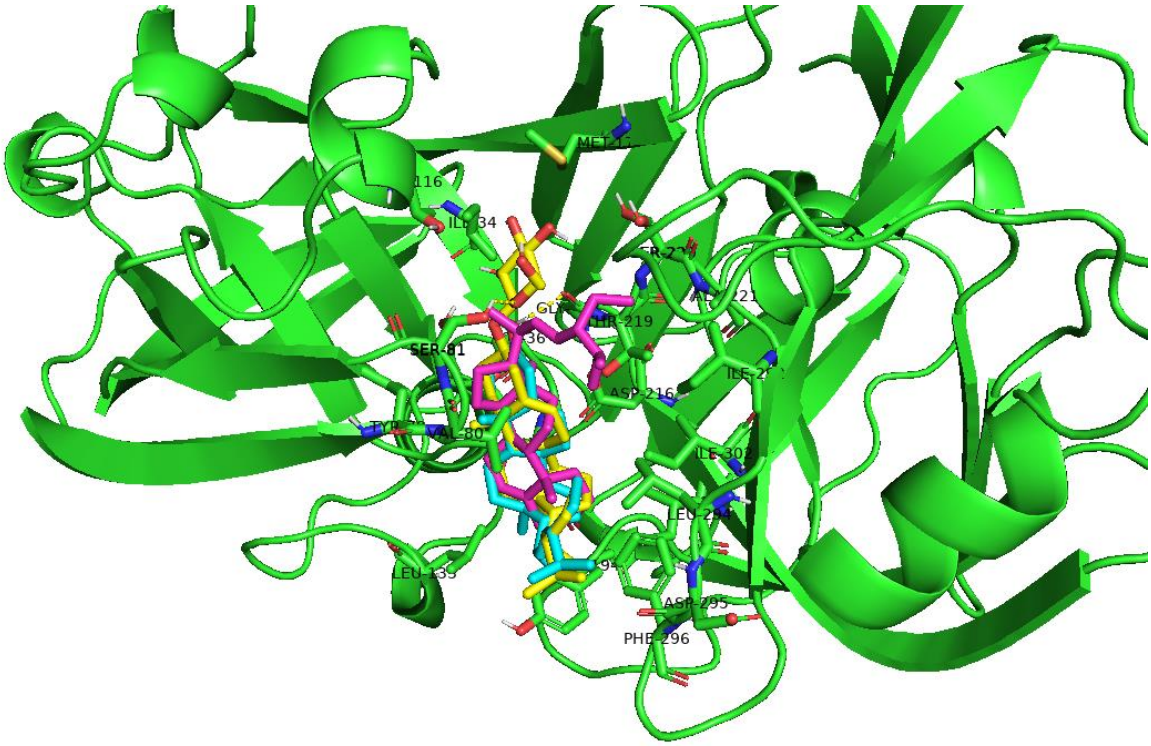

Figure 5: Compounds **1A** (cyan), **1B** (magenta) and **2C** (yellow) bound to plasmepsin II. Compounds **1A** and **2C** overlap in their conformations except for the sugar moiety of compound 2C.

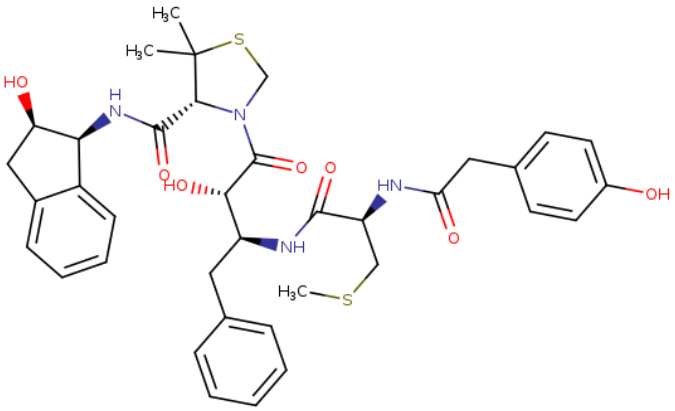

(4R)-N-[(1S,2R)-2-hydroxy-2,3-dihydro-1H-inden-1- yl]-3-[(2S,3S)-2-hydroxy-3-[(2R)-2-[2-(4-hydroxyphenyl)acetamido]-3-(methylsulfanyl)propanamido]-4-phenylbutanoyl]-5,5-dimethyl-1,3-thiazolidine-4-carboxamide (8V9 = peptidomimetic inhibitor of plasmepsin II)

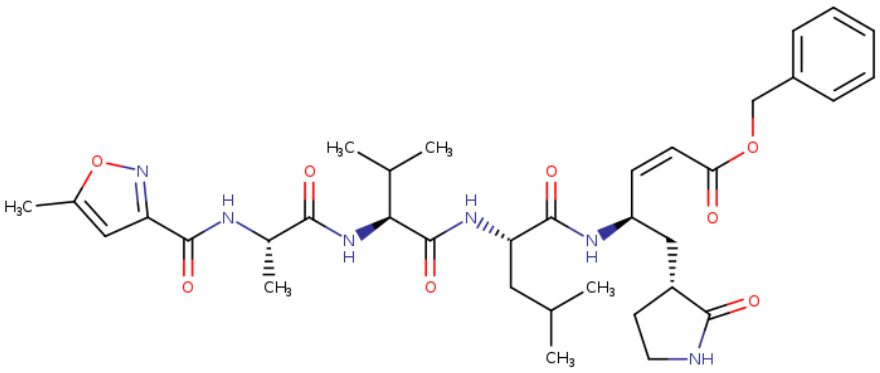

benzyl (2Z,4R)-4-[(2S)-4-methyl-2-[(2S)-3-methyl-2-[(2S)-2-[(5-methyl-1,2-oxazol-3-yl)formamido]propanamido]butanamido]pentanamido]-5-[(3R)-2-oxopyrrolidin-3-yl]pent-2-enoate (N3 = peptidomimetic inhibitor of SARS-COV-2 main protease)

Figure 6. The reference compounds for comparison in molecular docking calculations of plasmepsin II and SARS-COV-2 main protease, 8V9 and N3 respectively.

5. Conclusion

Three isolated phytoconstituents of a traditionally important plant, *Albizia zygia*, were screened against the plasmepsin II and main protease of SARS-CoV-2 by molecular docking. The docked compounds have a lower binding affinity and also interacted less with the plasmepsin II compared to the native ligand (also a known inhibitor).

The three compounds exhibited better affinity towards the main protease of SARS-CoV-2. The binding energy were -7.2, -6.5, -6.3 and -6.1 kcal/mol for stigmast-5,22-dien-3- O-glucopyranoside, 24-ethylcholest-5,22-dien-3-one, stigmast-5,22-dien-3-ol, and native ligand N3, respectively. The glycosylated steroid **2C,** having the highest binding energy and the most polar contacts relative to the native ligand and other test ligands, may therefore be considered for further *in vitro* and *in vivo* investigations.

Acknowledgments

The authors acknowledge the Central Science Laboratory, Obafemi Awolowo University, Ile-Ife, for access to some facilities for this project and Dr. Lukman O. Olasunkanmi for his assistance in running the NMR experiments.

References

1. B. B. Petrovska, Historical review of medicinal plants' usage. 2012, Pharmacogn. Rev. 6 (11), 1-5. doi: 10.4103/0973-7847.95849.
2. A. Ghorbani, Clinical and experimental studies on polyherbal formulations for diabetes: current status and future prospective. 2014, J. Intergr. Med. 12, 336–345. doi: 10.1016/S2095-4964(14)60031-5
3. WHO. WHO strategy on Traditional Medicine 2014–2023. 2013. https://www.who.int/medicines/publications/traditional/trm_strategy14_23en.
4. A. Sofowora, E. Ogunbodede, A. Onayade, The role and place of medicinal plants in the strategies for disease prevention. 2013, Afr. J. Tradit. Complement. Altern. Med. 10 (5), 210–229. doi: 10.4314/ajtcam.v10i5.2
5. S. O. Mintah, T. Asafo-Agyei, M. Archer, P. A. Junior, D. Boamah, D. Kumadoh, A. Appiah, A. Ocloo, Y. D. Boakye, C. Agyare, Medicinal plants for treatment of prevalent diseases. In: Pharmacognosy-Medicinal Plants; S. Perveen, A. Al-Taweel, Eds.; IntechOpen: London, UK, 2019. doi.org/10.5772/intechopen.82049.
6. R. J. Soares-Bezerra, A. S. Calheiros, N. C. da Silva Ferreira, V. da Silva Frutuoso, L. A. Alves, Natural products as a source for new anti-inflammatory and analgesic compounds through the inhibition of purinergic P2X receptors. 2013, *Pharmaceuticals*, 6 (5), 650-658. doi: 10.3390/ph6050650.
7. L. Zhang, N. Reddy, Bioactive Molecules from Medicinal Herbs for Life Threatening Diseases. 2018, J Mol Sci. 2, 4.
8. World Health Organization. World Malaria Report; WHO: Geneva, Switzerland, 2020; https://www.who.int/news-room/fact-sheets/detail/malaria
9. P. Chanda-Kapata, N. Kapata, A. Zumla. COVID-19 and malaria: A symptom screening challenge for malaria endemic countries. 2020, Int. J. Infect. Dis. 94, 151-153. doi.org/10.1016/j.ijid.2020.04.007
10. COVID-19 Coronavirus pandemic. https://www.worldometers.info/coronavirus/

11. OECD (2021). Policy Responses to Coronavirus (COVID-19). Coronavirus (COVID-19) vaccines for developing countries: An equal shot at recovery.
12. K. Kokila, S. D. Priyadharshini, V. Sujatha, Phytopharmacological properties of *Albizia* species: a review. 2013, Int. J. Pharm. Pharm. Sci. 5, 70–73.
13. M. A. Abdalla, H. Laatsch, Flavonoids from Sudanese *Albizia zygia* (*Leguminosae*, subfamily *mimosoideae*), a plant with antimalarial potency. 2012, Afr. J. Tradit. Complement. Altern. Med. 9, 56–58. doi: 10.4314/ajtcam.v9i1.8
14. O. P. Note, P. Chabert, D. E. Pegnyem, B. Weniger, M.-A. Lacaille-Dubois, A. Lobstein, Structure elucidation of new acacic acid-type saponins from *Albizia coriaria*. 2010, Magn. Reson. Chem. 48, 829–836. doi.org/10.1002/mrc.2671
15. Useful tropical plants. Tropical Plants Database, Ken Fern. tropical.theferns.info. (2021-11-04). <tropical.theferns.info/viewtropical.php?id=Albizia+zygia>
16. V. W. Kumbol, W. K. M. Abotsi, R. P. Biney, Antidepressant-like effect of *Albizia zygia* root extract in murine models. 2021, J. Basic Clin. Physiol. Pharmacol. 32 (1). doi.org/10.1515/jbcpp-2019-0310
17. G. K. Oloyede, A. O. Ogunlade, Phytochemical screening, antioxidant, antimicrobial and toxicity activities of polar and non-polar extracts of *Albizia zygia* (DC) Stem-Bark. 2013, Annu. Res. Rev. Biol. 3 (4), 1020-1031.
18. S.O. Okpo, S.M. Kporha, M. C. Chijioke, Gastro-protective potential of aqueous stem bark extract of *Albyzia zygia* in rat models of ulcer. 2016, J. Pharm. Allied Sci. 13, 2309-2318.
19. S. B. Lamptey, W. K. M. Abotsi. *Albizia zygia* (DC.) Macbr. Hydroethanol root extract exerts anti-Oedemic and in vivo antioxidant activities in animal models. 2017, J. Appl. Pharm. Sci. 7 (4), 199-205. doi: 10.7324/JAPS.2017.70429
20. R. Appiah-Opong, I. K. Asante, D. O, Safo, I. Tuffour, E. Ofori-attah, T. Uto, A. K. Nyarko, Cytotoxic effects of *Albizia zygia* (DC) JF Macbr, a Ghanaian medicinal plant, against human T-lymphoblast-like leukemia, prostate and breast cancer cell lines. 2016, Int. J. Pharm. Pharm. Sci. 8 (5), 392-396.
21. W. K. M. Abotsi, S. B. Lamptey, S. Afrane, E. Boakye-Gyasi, R. U. Umoh, E. Woode, An evaluation of the anti-inflammatory, antipyretic and analgesic effects of hydroethanol leaf extract of *Albizia zygia* in animal models. 2017, Pharm. Biol. 55 (1), 338-348, doi: 10.1080/13880209.2016.1262434
22. P. Amoateng, D. Osei-Safo, K. K. E. Kukuia, S. Adjei, O. A. Akure, C. Agbemelo-Tsomafo, S. N. Adu-Poku, K. Y. Agyeman-Badu, Psychotropic Effects of an

Alcoholic Extract from the Leaves of *Albizia zygia* (*Leguminosae-Mimosoideae*). 2017, Evid.-based Complement. Altern. Med. ID: 9297808. doi:10.1155/2017/9297808

23. N. P. Okoye, O. Idah, T. O. Ogundeko, L. N. Kamoh, S. M. C. Ramyil, K. Amadi, B. Modupe, Gastrointestinal transit of aqueous and crude leaf extracts of *Albizia zygia* in male albino rats. 2021, Int. J. Pharm. Pharm. Res. 22 (2), 78-87.
24. A. A. Olarbi, E. O. Bekoe, C. Agyare, N. Osafo, V. E. Boamah, In vivo anti-inflammatory and antioxidant properties of *Albizia zygia* D. C. Macbr. 2016, Planta Med. 82 (S 01), S1-S381. doi: 10.1055/s-0036-1596353
25. O. D. Olukanni, E. Lugard, E. Emmanuel, A. T. Olukanni, F. Ayoade, E. U. Durugbo, Antioxidant and in vitro anti-inflammatory activities of *Albizia zygia* (DC) J.F. mebr and the evaluation of its phytochemical constituents. 2020, J. Med. Plants Stud. 8 (4), 317-323
26. B. L. Ndjakou, B. Weniger, F. Tantangmo, M. Chaabi, S. Ngouela, E. Tsamo, R. Anton, Antimalarial and antitrypanosomal activities of West Cameroon medicinal plants. 2006, Planta Med., 72 (11), P_008. doi: 10.1055/s-2006-949808.
27. T. Schoppa, P. Pachaly, Inhaltsstoffe von *Albizzia zygia*. 1981, Arch. Pharm. (Weinheim) 314 (1), 18–25.
28. P. Pachaly, F. Redeker, T. Schoppa, Inhaltsstoffe von *Albizzia zygia*, 2. 1983, Arch Pharm. (Weinheim) 316 (7), 651–652.
29. O. P. Noté, L. Simo, J. N. Mbing, D. Guillaume, S. A. Aouazou, C. D. Muller, D. E. Pegnyemb, A. Lobstein, Two new triterpenoid saponins from the roots of *Albizia zygia* (DC.) J.F. Macbr. 2016, Phytochem Lett. 18:128–135.
30. O. P. Noté, L. M. Simo, J. N. Mbing, D. Guillaume, C. D. Muller, D. E. Pegnyemb, A. Lobstein, Structural determination of two new acacic acid-type saponins from the stem barks of *Albizia zygia* (DC.) JF Macbr. 2019, Nat. Prod. Res. 33 (2), 180-188. doi.org/10.1080/14786419.2018.1440228
31. M. A. Abdalla, H. Laatsch, Flavonoids from Sudanese *Albizia zygia* (*Leguminosae,* subfamily *Mimosoideae*), a plant with antimalarial potency. 2012, Afr. J. Tradit. Complement. Altern. Med. 9 (1), 56–58. doi: 10.4314/ajtcam.v9i1.8
32. R. R. Koagne, F. Annang, B. Cautain, J. Martin, G. Peres-Moreno, G. Bitchagno, D. Gonzalez-Pacanowska, F. Vicente, I. K. Simo, F. Reyes, P. Tane, Cytotoxicity and antiplasmodial activity of phenolic derivatives from *Albizia zygia* (DC.) J.F. Macbr.

(*Mimosaceae*). 2020, BMC Complement. Med. Ther. 20 (1), 8. https://doi.org/10.1186/s12906-019-2792-1

33. Z. N. Aiezzah, E. Noor, M. S. Hasidah, Suppression of *Plasmodium berghei* parasitemia by LiCl in an animal infection model. 2010, Trop. Biomed. 27 (3), 624-631.
34. D. J. Knight, W. Peters, The antimalarial activity of N-benzyloxydihydrotriazines: I. The activity of clociguanil (BRL 50216) against rodent malaria, and studies on its mode of action. 1980, Ann. Trop. Med. Parasitol., 74 (4), 393-404.
35. T. O. Elufioye, J. M. Agbedahunsi, Antimalarial activities of *Tithonia diversifolia* (Asteraceae) and *Crossopteryx febrifuga* (Rubiaceae) on mice in vivo. 2004, J. Ethnopharmacol. 93 (2), 167-171. doi: 10.1016/j.jep.2004.01.009
36. O. Trott, A.J. Olson, AutoDock Vina: improving the speed and accuracy of docking with a new scoring function, efficient optimization and multithreading. 2010, J. Comput. Chem. 31, 455-61. doi: 10.1002/jcc.21334
37. O. A. Fadare, E. O. Iwalewa, C. A. Obafemi, F. P. Olatunji. In-silico antimalarial study of monocarbonyl curcumin analogs and their 2,4-dinitrophenylhydrazones using the inhibition of Plasmepsin II as test model. 2017, Am. J. Pharmacol. Sci. 5 (2), 18-24. doi: 10.12691/ajps-5-2-1
38. V. S. P. Chaturvedula, I. Prakash, Isolation of stigmasterol and β-sitosterol from the dichloromethane extract of *Rubus suavissimus*. 2012, Int. Curr. Pharm. J. 1 (9), 239-242. doi.org/10.3329/icpj.v1i9.11613
39. P. Georges, M. Sylvestre, H. Ruegger, P. Bourgeois, Ketosteroids and hydroxyketosteroids, minor metabolites of sugarcane wax. 2006, Steroids 71 (8), 647-652. doi.org/10.1016/j.steroids.2006.01.016
40. A. Syafrinal, E. Mai, Isolation and elucidation structures of stigmasterol glycoside from *Nothopanax scutellarium* Merr leaves. 2015, J. Chem. Pharm. Res. 7 (12), 763-765.
41. A. Ridhay, A. Noor, N. H. Soekamto, T. Harlim, I. V. Altena, A stigmasterol glycoside from the root wood of *Melochia Umbellata* (Houtt) Stapf *var*. degrabrata K. 2012, Indo. J. Chem. 12 (1), 100-103.
42. J. B. Harborne, Phytochemical methods: A guide to modern techniques of plant analysis. 3rd edition, Chapman and Hall, London, 1998, pp 74-83.

43. A. U. Krettli, J. O. Adebayo, L. G. Krettli, Testing of natural products and synthetic molecules aiming at new antimalarials. 2009, Curr. Drug Targets. 10 (3), 261–270. doi:10.2174/138945009787581203.
44. S. S. Muttaqin, J. S. Maji, Screening of oxamic acid similar 3D structures as candidate inhibitor *Plasmodium falciparum* L-lactate dehydrogenase of malaria through molecular docking. 2018, 1st International conference on bioinformatics, biotechnology, and biomedical engineering - bioinformatics and biomedical engineering, pp 1-6. doi: 10.1109/BIOMIC.2018.8610537.